Hexakis Porphyrinato Benzenes. A New Class of Porphyrin Arrays

H. A. M. Biemans,[†] A. E. Rowan,*[,‡] A. Verhoeven,[‡] P. Vanoppen,[§] L. Latterini,[§] J. Foekema,[‡] A. P. H. J. Schenning,[†] E. W. Meijer,[†] F. C. de Schryver,[§] and R. J. M. Nolte[‡]

Contribution from the Department of Organic Chemistry, NSR Center, University of Nijmegen, The Netherlands, the Department of Macromolecular and Organic Chemistry, Eindhoven University of Technology, The Netherlands, and the Department of Chemistry, Katholieke Universiteit of Leuven, Belgium

Received May 4, 1998

Abstract: A new type of porphyrin array has been synthesized by the coupling of six porphyrin moieties to a central benzene core via an ether linkage. The resulting porphryin supermolecule has a diameter up to 80 Å and a mass of 8500 daltons. In solution, the six porphyrins around the central benzene ring arrange themselves into three sets of offset overlapping dimers, which are rapidly interconverting at room temperature. Solution UV−vis and fluorescence studies, however, indicate that there are no electronic interactions between the individual porphyrin molecules. Upon spreading a chloroform solution of these porphyrin molecules on a surface, they self-assemble to form ring-shaped architectures on a micrometer scale. Near-field scanning optical microscopy studies reveal that the porphyrin moieties within the rings have an ordered arrangement with respect to their position in the ring after the sample has been annealed at 80 °C for 2 days.

Introduction

The design and construction of novel porphyrin architectures, in particular well-defined porphyrin arrays, is an area of increasing current interest.[1−3] These porphyrin assemblies are of fundamental importance not only as models for the study of the energy and electron-transfer functions of the light-harvesting antenna and the photosynthetic reaction centers but also as building blocks for the construction of functional molecular devices, i.e., molecular scale wires, switches and photovoltaic devices, etc.[1,4] In the case of the natural antenna systems, the function and properties of the chromophoric arrays are controlled by the spatial arrangement and orientation of the molecules, which themselves are held in a specific architecture through predominantly noncovalent interactions within a protein and carotenoid scaffold. The resulting assemblies, which can consist of up to several hundred porphyrins, are able to transfer energy over large distances with a very high efficiency.[5,6] More recently, the crystal structure of the light-harvesting antenna LH2 of a purple photosynthetic bacterium was resolved.[6] In this antenna complex, the bacteriochlorophyll chromophores are arranged into two sets of rings which are formed by the self-assembly of nine identical components. The first step toward mimicking the properties of such systems is the development of techniques which enable the construction of well-defined multichromophore arrays.[7]

In earlier work, we have been focused in particular on the design of cyclic arrays of porphyrins for the study of through-space electron transfer and of simple synthetic architectural mimics of the antenna complex LH2. It was shown that large ring-shaped assemblies of porphyrins can be formed by spreading and evaporating a thin film of a chloroform solution of the

[†] Department of Macromolecular and of Organic Chemistry, Eindhoven University of Technology.

[‡] Department of Organic Chemistry, NSR Center, University of Nijmegen.

[§] Department of Chemistry, Katholieke Universiteit of Leuven.

(1) Wagner, R. W.; Lindsey, J. S. *J. Am. Chem. Soc.* **1994**, *116*, 9759; Wagner, R. W.; Johnson, T. E.; Lindsey, J. S. *J. Am. Chem. Soc.* **1996**, *118*, 11167. Hsiao, J.-S; Krueger, B. P.; Wagner, R. W.; Johnson, T. E.; Delaney, J. K.; Mauzerall, D. C.; Fleming, G. R.; Lindsey, J. S.; Bocian, D. F.; Donohoe, R. J. *ibid* **1996**, *118*, 11181. Seth, J.; Palaniappan, V.; Wagner, R. W.; Johnson, T. E.; Lindsey, J. S.; Bocian, D. F. *ibid* **1996**, *118*, 11194. Wagner, R. W.; Lindsey, J. S.; Seth, J.; Palaniappan, V.; Bocian, D. F. *ibid* **1996**, *118*, 3996. Hsiao, J.-S; Krueger, B. P.; Strachan, J.-P.; Gentemann, S.; Seth, J.; Kalsbeck, W. A.; Lindsey, J. S.; Holten, D.; Bocian, D. F. *ibid* **1997**, *119*, 11191.

(2) Officer, D. L.; Burrell, A. K.; Reid, D. C. W. *Chem. Commun.* **1996**, 1657.

(3) Osuka, A.; Liu, B.; Maruyama, K. *J. Org. Chem.* **1993**, *58*, 3582. Sessler J. L.; Capuano, V. L.; Harriman, A. *J. Am. Chem. Soc.* **1993**, *115*, 4618−4628; Kawabata, S.; Yamazaki, I.; Nishimura, Y.; Osuka, A. *J. Chem. Soc., Perkin Trans. 2*, **1997**, 479.

(4) Drain, C. M.; Russell K. C.; Lehn J-M. *Chem. Commun.* **1996**, 337; Drain, C. H.; Lehn, J.-M. *J. Chem. Soc., Chem. Commun.* **1994**, 2313.

(5) Deisenhofer, J.; Epp, O.; Miki, K.; Huber, R.; Michel, H. *Nature* **1985**, *318*, 618. Feher, G.; Allen, J. P.; Allen, M. Y.; Okamura, Y.; Rees, D. C. *Nature* **1989**, *339*, 111.

(6) McDermott, G.; Prince, S. M.; Freer, A. A.; Hawthornthwaite-Lawless, A. M.; Papiz, M. Z.; Codgell, R. J.; Isaacs, N. W. *Nature* **1995**, 517; Isaacs, N. W.; Codgell, R. J.; Freer, A. A.; Prince, S. M. *Curr. Opin. Struct. Biol.* **1995**, *5*, 794.

(7) For recent reviews of porphyrin assemblies and arrays, see; Chin-Ti, C. *Comprehensive Supramolecular Chemistry*; Pergamon Press: Elmsford, NY, 1996; Vol. 5, No. 4, pp 91−140. Sanders, J. K. M. *Comprehensive Supramolecular Chemistry*; Pergamon Press: Elmsford, NY, 1996; Vol. 9, No. 4, pp 131−164. Ward, M. D. *Chem. Soc. Rev.* **1997**, *26*, 365. Harriman, A.; Sauvage J.-P. *Chem. Soc. Rev.* **1996**, *25*, 41. Krishna Kumar, R.; Balasubramanian, S.; Goldberg, I. *Inorg. Chem.* **1998**, *37*, 541−552; Chambron J.-C.; Dietrich-Buchecker, C. O.; Heitz, V.; Sollardie, N.; Sauvage J−P. *C. R. Acad. Sci.* **1996**, 483. Solladie, N.; Chambron J.-C.; Dietrich-Buchecker, C. O.; Sauvage J−P. *Angew. Chem., Int. Ed. Engl.* **1996**, *35*, 906. Shimidu, T. *Synth. Met.* **1996**, *81*, 235. Osuka, A.; Shimidzu, H. *Angew. Chem., Int. Ed. Engl.* **1997**, *1*, 1135. Ogawa T.; Nishimoto Y.; Yoshida N.; Ono N.; Osukua, A. *Chem. Commun.* **1998**, 337. Liu H−Y.; Huang, J.-W.; Tian, X.; Jiao, X.-D.; Luo, G.-T.; Ji, L.-N. *Chem. Commun.* **1997**, 1575. Burrell, A. K.; Officier, D. L.; Reid, D. C. W.; Wild, K. Y. *Angew. Chem., Int. Ed. Engl.* **1998**, *37*, 114. Anderson, H. L. *Inorg. Chem.* **1994**, *33*, 972. Jiang, B.; Yang S−W.; Barbini, D. C.; Jones W. E. *Chem. Commun.* **1998**, 213. Hunter, C. A.; Hyde, R. K. *Angew. Chem., Int. Ed. Engl.* **1996**, *35*, 1936. Drain C. H.; Lehn, J.-M. *J. Chem. Soc., Chem. Commun.* **1994**, 2313. Alessio, E.; Macchi, M.; Heath, S.; Marzilli, L. G. *Chem. Commun.* **1996**, 2313.

10.1021/ja9815632 CCC: $15.00
Published on Web 10/16/1998

Scheme 1

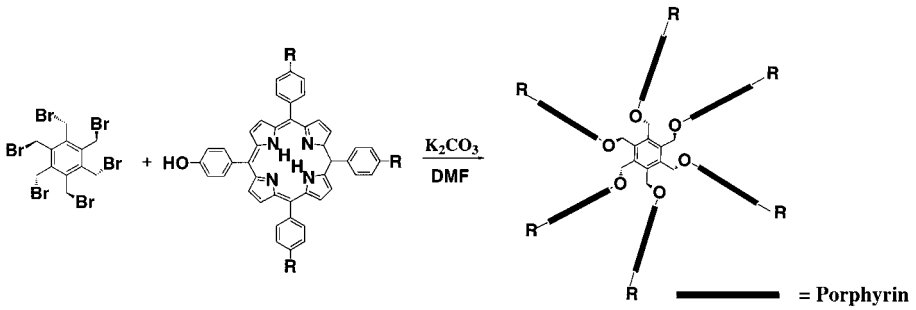

2 a, R = CH_3
b, R = $OC_{16}H_{33}$

5 a, R = CH_3
b, R = $OC_{16}H_{33}$

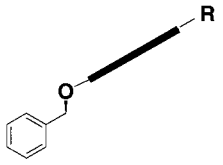

3, R = $OC_{16}H_{33}$

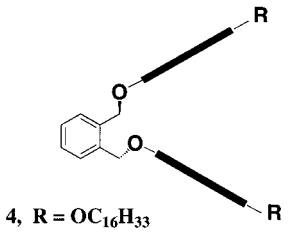

4, R = $OC_{16}H_{33}$

metal porphyrin dimer **1** on a substrate.[8] More recent photo-

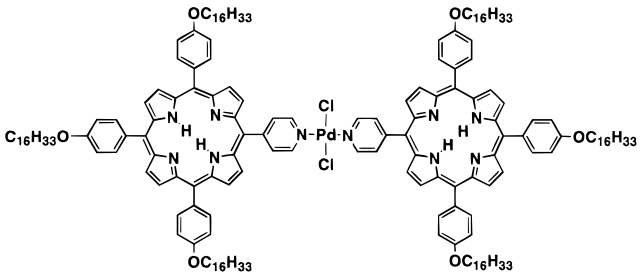

1

physical investigations of the formed porphyrin rings using confocal microscopy, atomic force microscopy, and near-field scanning optical microscopy (NSOM) showed that the nanosized rings did not consist of a highly ordered arrangement of porphyrins but were constructed from a conglomerate of smaller nanosized porphyrin aggregates.[9] To increase the organization within the rings it was decided to synthesize larger porphyrin-containing moieties which might still assemble into nanosized rings but in a more ordered arrangement. In principle, a larger porphyrin 'surface' should result in greater intermolecular interactions and, hence, increased order upon aggregation. Several authors have recently described the synthesis and investigation of large multiporphyrin-containing molecules (trimeric,[1] pentameric,[2] and even nonomeric[3] porphyrin molecules) but have not studied the self-assembling behavior of such species. Reported herein is the construction and study of a new type of hexameric porphyrin molecule in which all of the chromophores are anchored to one central benzene ring (Scheme 1) in order to form a large disc-shaped porphyrin surface. This porphyrin supermolecule can self-assemble to generate micrometer-sized rings which have been studied by NSOM.

Results and Discussion

The porphyrin derivatives **3**, **4**, **5a**, and **5b** were synthesized by base-catalyzed coupling reactions. The reaction of hexakis-(bromomethyl)benzene and porphyrins **2a** and **2b**[7] gave the porphyrin arrays **5a** and **5b** in good yields (Scheme 1). Surprisingly, only one product, (the hexasubstituted species)[10] was obtained from the reaction in addition to the recovered starting material. Even when only 1 equiv of porphyrin per hexakis(bromomethyl)benzene was used, the only product was that of the hexasubstituted benzene. This remarkable selectivity of product formation suggests a significant templating effect of a porphyrin already attached to the central ring, upon the coupling of a second and subsequent porphyrin species, probably through $\pi-\pi$ stacking interactions. The two hexameric porphyrins **5a** and **5b** were fully characterized by elemental analysis and ^{1}H NMR spectroscopy. According to molecular modeling calculations, these hexameric species have nanometer dimensions with a calculated width of 48 Å for **5a** and 84 Å for **5b**. High-resolution mass spectroscopy further highlighted the superstructure of these species, showing correct peaks for both compounds viz. $M^+ = 4178.78$ [$C_{294}H_{222}N_{24}O_6$] for **5a** and $M^+ = 8266.73$ [$C_{564}H_{762}N_{24}O_{24}$] for **5b,** respectively. The monoporphyrin and bis porphyrin compounds **3** and **4** were obtained by the same reaction as that of **5a** and **5b** but with benzyl bromide and α,α'-dibromo-*o*-xylene as the starting compounds, respectively.

The ^{1}H NMR spectrum (300 MHz) of the single porphyrin compound complex **3** showed that the porphyrin moiety was

(8) Schenning, A. P. K. J.; Benneker, F. B. G.; Geurts, H. P. M., Liu X. Y.; Nolte, R. J. M. *J. Am. Chem. Soc.* **1996**, *118*, 8549.

(9) Hofkens, J.; Latterini, L.; Vanoppen, P.; Faes, H.; Jeuris, K.; De Feyter, S.; Kerimo, J.; Barbara, P. F.; De Schryver, F. C.; Rowan, A. E.; Nolte, R. J. M. *J. Phys. Chem.* **1997**, *101*, 10588−10598.

(10) A similar hexakis(ruthenium bipyridine)benzene array has been initially reported by: Constable, E. C.; P. Harverson *Chem. Commun.* **1996**, 33. Constable, E. C. *Chem. Commun.* **1997**, 1073. Constable, E. C.; P. Harverson *Inorg. Chem. Acta* **1996**, *252*, 281.

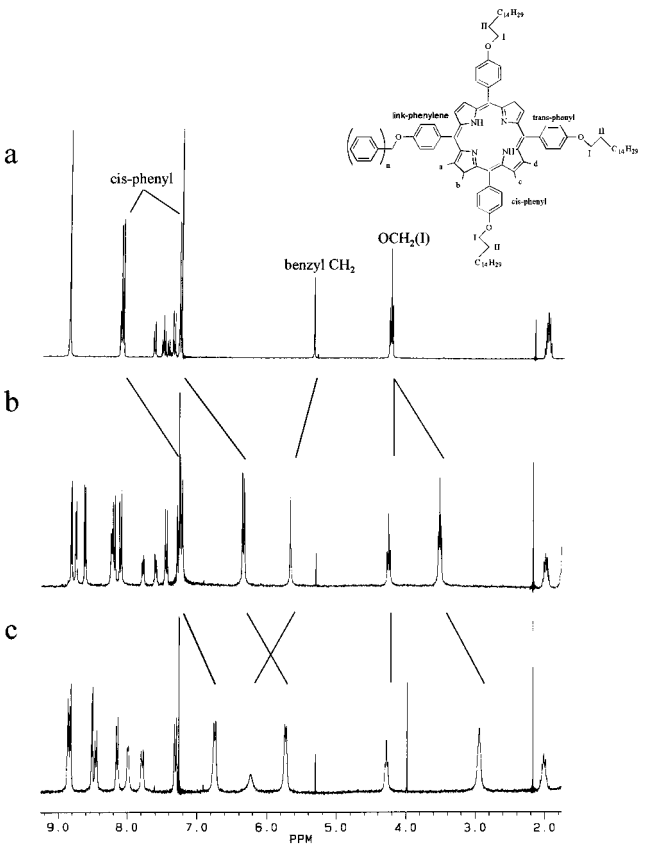

Figure 1. ^{1}H NMR (300 MHz, $CDCl_3$, concentrated 1×10^{-3} M) spectra of monoporphyrin **3** (a), bis porphyrin **4** (b), and hexakis porphyrin **5b** (c). Highlighted are the resonances that most clearly demonstrate the increase in asymmetry upon the increase in the number of porphyrin moieties.

symmetrical in the sense that all of the pyrrolic protons displayed the same chemical shift as did the protons of the attached phenyl groups (Figure 1a). Upon the addition of a neighboring porphyrin, as in **4**, this symmetry was disrupted as can be seen from the ^{1}H NMR spectrum in Figure 1b, in which upfield shifts are observed for several resonances of the porphyrin moiety due to the effect of the ring current of the neighboring porphyrin ring. The largest shifts occur for the resonances of the *cis*-phenyl protons which are shifted upfield by 0.89 ppm (ortho) and 0.91 ppm (meta) (see Table S1, Supporting Information). In addition, there are large upfield shifts for the pyrrolic protons b and c (see Figure 1b). The porphyrin molecule is now magnetically dissymmetric. Since only one AB pattern is seen for the two sets of *cis*-phenyl protons, it is clear that the bis porphyrin is rapidly interconverting between two equivalent states and the observed shifts are averaged values for the two halves of the porphyrin.

The ^{1}H NMR spectrum of **5b** revealed even larger ring-current shifts than those seen for the bis porphyrin **4** (Table S1 Supporting Information, Figure 1c), while the tolyl derivative **5a** displayed ring-current shifts ($\Delta\delta$'s compared to the monomeric species **3**) almost identical to those of compound **4**, suggesting a similar orientation of the porphyrin moieties. In the case of hexamer **5b** the ring shifts were approximately twice as large as those of the bis porphyrin. Although larger, the relative shifts were very similar. Again, the largest shifts were observed for the *cis*-phenyl protons ($\Delta\delta$'s ortho $= -1.37$ ppm and $\Delta\delta$'s meta $= -1.52$ ppm) and for the CH_2 protons (I and II) of the attached oxyalkyl tails which were also shifted substantially upfield ($\Delta\delta$'s CH_2(I) $= -1.3$ ppm and $\Delta\delta$'s CH_2(II) $= -0.5$ ppm, (see Table S1, Figure 1c). The pyrrole protons also feel the nearby porphyrin rings, in particular the b and c protons which are both shifted upfield by -0.88 ppm and -0.36 ppm, respectively. In contrast, the protons which are situated between the porphyrin and the central benzene core were all moved downfield, indicating that they feel the side of the aromatic surface. In the case of the protons of the *p*-phenylene ring linking the porphyrins and the core the shifts were $\Delta\delta$'s $+0.34$ and $\Delta\delta$'s $+0.43$ for the ortho (to the porphyrin) and meta protons, respectively. These shifts were not seen for compound **3**. As one goes from the mono to the bis to the hexakis porphyrin, the benzylic CH_2 resonance moves stepwise downfield (**3** $\delta = 5.34$ ppm; **4** $\delta = 5.67$ ppm, **5b** $\delta =$ 6.22 ppm), which in combination with the observed increase in broadening indicates a decrease in conformational freedom. Assuming that the oxymethylene connection to the central benzene ring adopts an alternating up−down conformation,[11] according to molecular modeling studies (Quanta CHARMM 3.3) the center-to-center distance is approximately 10−12 Å if the porphyrin molecules are fully separated and orthogonal to the central benzene ring. Since the porphyrin moieties feel the ring currents of an adjacent porphyrin, they must be, at some time, closer. A 2D NOESY spectrum of the hexameric species **5b** revealed several large correlations between the porphyrin central NH protons and protons at the porphyrin periphery which cannot be intramolecular correlations and, hence, must be due to intermolecular interactions with a porphyrin neighbor (Figure S2, Supporting Information). A 2D NOESY spectrum was also recorded for compound **4**; however, no NOE correlations to the central porphyrin NH protons were observed. Analysis of the NOE interactions for **5b** revealed a geometry in which one of the *cis*-phenyl groups is directly over the center of a neighboring porphyrin ring. From the observed NOEs, ^{1}H NMR ring-current shifts, and the molecular modeling studies, we propose that the hexakis porphyrin species exists as three porphyrin pairs, in which each pair adopts a geometry similar to that of the simple bis porphyrin species **4** (Figure 2). (This geometry is similar to that observed for the hydrogen bonding hexaporphyrin species reported by Lehn et al).[4] The three sets of porphyrin pairs in **5b** rapidly interconverting on the NMR time scale (see Figure 2b).[12]

Comparison of the UV−vis spectra of chloroform solutions of **3**, **4**, and **5b** showed no differences in the absorption spectra, except for a very slight broadening of the Soret band for the

(11) It should be noted that the substituents on the benzene ring can adopt a variety of conformations. In general the alternating *ababab* conformation is the most common, see McNicol, D. D.; Downing G. A. *Comprehensive Supramolecular Chemistry*; Pergammon Press: Elmsford, NY, 1996; Vol. 6, No. 17, pp 421. Marx, H. W.; Moulines, F.; Wagner, T.; Astruc, D. *Angew. Chem., Int. Ed. Engl.* **1996**, *35*, 1701.

(12) To investigate this interconversion process in more detail, variable temperature ^{1}H NMR (400 MHz, $CDCl_3$) experiments were performed with molecule **5b**. As the temperature was decreased (0 to -10 °C), significant line broadening was seen for the signals of the two pyrrole protons a and b, the *cis*-phenyl protons and the CH_2O protons of the *cis*-alkoxy phenyl rings. At -20 °C, both the a and b pyrrole protons were too broad to be observed; the CH_2O resonance of the *cis*-tails, however, was observed to split into two peaks. In addition, the *cis*-phenyl protons, which at room temperature gave an AB pattern, also split with each proton having two resonances. As the temperature was further lowered to -40 °C, no other resonances were found to coalesce or broaden significantly. The resonances which split exhibited similar behavior, with one of the peaks gradually moving upfield and the other one slowly moving downfield (at -30 °C the ortho *cis*-phenyl = 5.96, 5.22 ppm; meta *cis*-phenyl 7.00, 6.25 ppm; CH_2O of *cis*-alkoxyphenyl = 3.00, 2.48 ppm). The coalescence occurred at -15 °C and is not a simple slowing of rotation around the *cis*-alkoxyphenyl moieties since this would not be expected to affect the pyrrole protons and the *cis*-CH_2O resonance. The observed process is therefore attributed to the interconversion between dimeric pairs (Figure 2b).

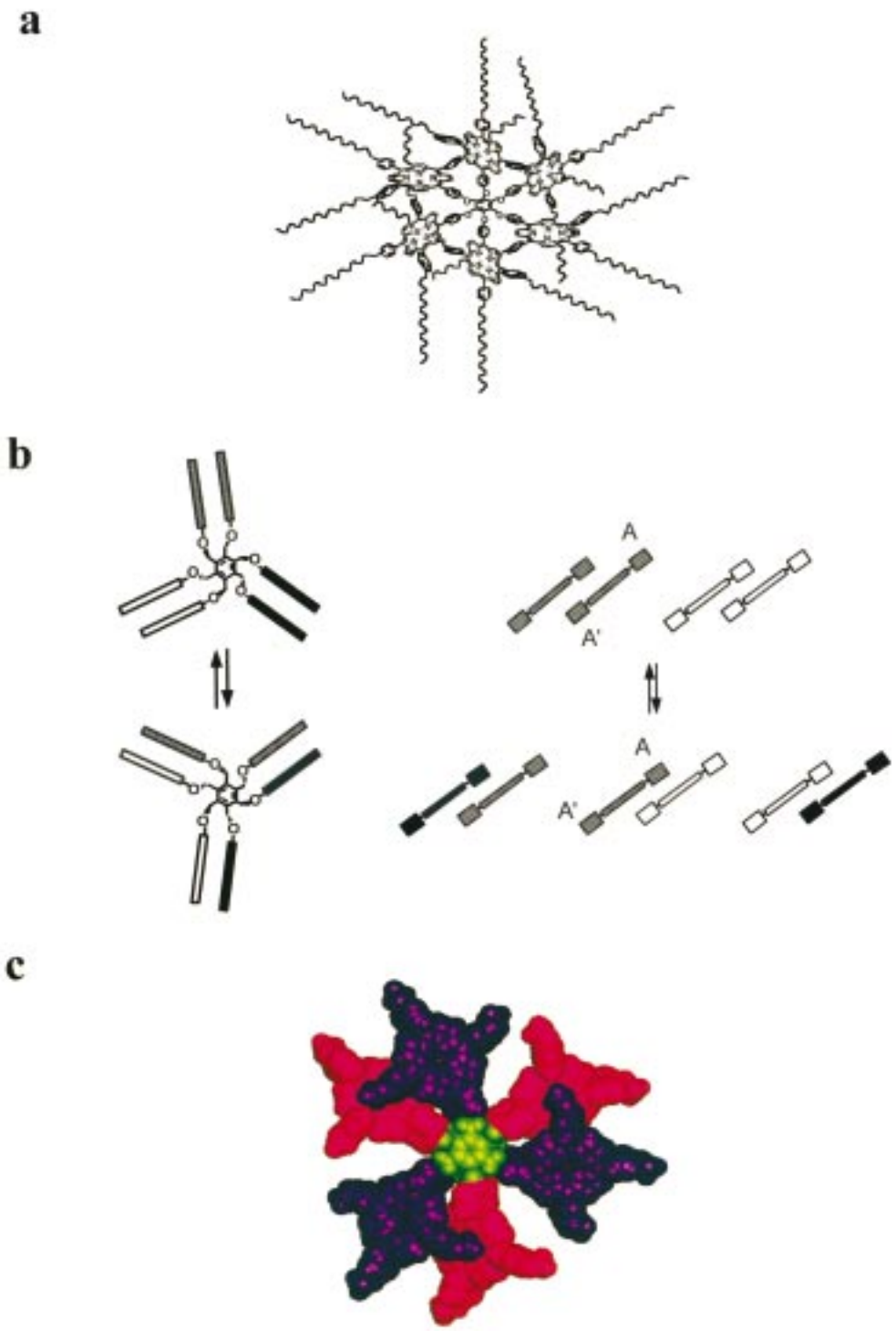

Figure 2. (a) Drawing of the hexakis porphyrin molecule **5b**. (b) Schematic representation of the dimer interconversion for compound **5b**; top view and side view showing the interconversion of the two *cis*-phenyls A and A′ which is frozen out at −15 °C resulting in inequivalence (^{1}H NMR, 400 MHz). (c) Calculated geometry for **5b** as derived from the ^{1}H NMR studies (van der Waals model, QUANTA, CHARMM 3.3 force field).

hexasubstituted derivatives **5.**[13] Single-photon time measurements performed on **3**, **4**, and **5b** in benzene solution (excitation at 418 nm, 298 K) showed fluorescence monoexponential decays with $\tau_f = 8.1$, 8.3, and 8.2 ns, respectively, further confirming the lack of electronic interaction between adjacent porphyrin molecules seen in the UV−vis spectra. In the case of the tolyl derivative **5a** in chloroform (by exciting at 420 nm), a fluorescence monoexponential decay with $\tau_f = 3.8$ ns was observed. In the more viscous solvent 1,3,5-trichlorobenzene, the decay remained monoexponential, but the decay time became longer, $R_f = 8.0$ ns, suggesting a very small interaction between the porphyrin rings. When **5a** was cooled in 2-methyltetrahydrofuran below the onset of the glassy phase (77 K), the excitation spectrum changed dramatically with the Soret band

(13) Several authors have studied the electronic interactions between porphyrins directly attached to a benzene ring and found that interactions are predominantly through bond and not through space.[3,4] In the case of the hydrogen bonding hexamer of Lehn, a slight red shift in the Soret band was observed upon formation of the hexaporphyrin species.

clearly splitting into two components. This observed splitting is indicative of electronic interactions between the porphyrin rings within **5a**. The lack of significant electronic interaction in **5b** and to a lesser extent in **5a** at first glance appears to be contradictory with the ^{1}H NMR data. However, according to molecular modeling the center-to-center distance between two porphyrin rings in an offset stacking geometry in molecule **5** is 9 Å, which is too large for any significant exciton coupling to occur between neighboring porphyrin π-systems. To further investigate the geometric arrangement within the hexakis porphyrin species, the respective copper compounds **Cu·3**, **Cu·4**, and **Cu·5b** were synthesized. EPR spectroscopy studies were carried out with chloroform solutions of all three species at 298 and 77 K (1×10^{-3} M). As in the photophysical studies no interactions were observed between the unpaired electrons of the metal centers of the two neighboring porphyrin units suggesting that the copper−copper distances are larger than 6 Å, even in the frozen state at 77 K.

In an earlier paper, we have shown that nanometer to microscale ring-shaped assemblies of porphyrins can be formed by allowing thin films of a porphyrin solution to evaporate on a substrate.[9] The same physical phenomenon was later found to also lead to the formation of large rings of Ag nanoparticles[14] and could in part be responsible for the perfect rings formed by carbon nanotubes.[15] To more fully understand the process of ring formation and investigate the internal architecture of the porphyrin nanorings, we have carried out photophysical investigations using confocal microscopy, atomic force microscopy, and NSOM. It was found that in the case of molecule **1** the ring-shaped assemblies were not ordered arrays of porphyrin molecules but consisted of a conglomerate of smaller nanosized porphyrin aggregates. The original aims of synthesizing the hexakis-substituted benzene derivatives **5** was to generate large porphyrin compounds which might also assemble into nanosized rings but in a more ordered arrangement. Spreading of a chloroform solution of the free base hexasubstituted derivative **5b** (10^{-6} M) on a substrate (carbon surface or a glass slide) consistently resulted in the formation of wheel-like assemblies similar to those previously described.[8] The rings differed from those described previously, in that the average diameter of the rings formed by **5b** is larger, with rings of up to 27 μm across being formed (see Figure 3a). The rings reported previously only varied from 1 to 5 μm in diameter. In general the larger the diameter of the ring, the larger the thickness of the ring.[8] The morphology of the rings was initially investigated by UV−vis spectroscopy on a film spread on a glass substrate. The Soret band of the porphyrin moieties in the film was found to be red-shifted by 10 nm in comparison to the position of the Soret band in chloroform solution. No red shift could be observed in solution at higher concentrations (it should be noted that due to the large extinction coefficient of molecule **5b**, only concentrations of up to 1×10^{-5} M could be measured). The red shift observed is similar to that seen for the films formed from molecule **1** and is suggestive of an offset stacking geometry in the aggregate. This red shift observed for a film formed from **5b** could be due either to a change in geometry of the porphyrins within a single molecule or to intramolecular exciton coupling which arises upon aggregation. A variety of hexakis-substituted benzene derivatives have been shown to be excellent discotic mesogens and to form well-defined discotic thermotropic liquid-crystalline phases.[16] The mesogenic behavior of **5b** was initially investigated by polarizing microscopy and a thermotropic liquid−crystalline phase was observed between 140 and 190 °C, which is presumed to be a discotic mesophase. This liquid−crystalline phase implies a pronounced intermolecular interaction between the molecules. In the hope of utilizing these interactions in order to increase the ordering within the rings, we therefore annealed the formed rings in an oven at 80 °C for 2 days.

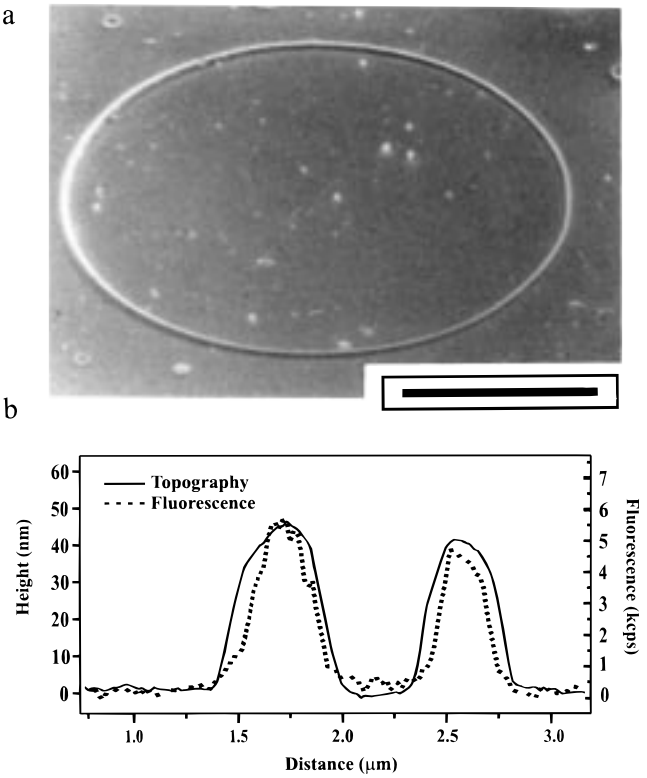

Figure 3. Scanning electron microscope picture of the ring-shaped assemblies formed by evaporation of a thin film of hexakis porphyrin compound **5b** in chloroform on a carbon substrate concentrated 1×10^{-5} M, bar = 10 μm). (b) NSOM topological and fluoresence line image of a slice through the rings formed from thin films (concentrated 1×10^{-6} M) of **5b** in chloroform on a glass substrate, revealing the correlation between the topology and fluorescence.

NSOM was used to investigate both the morphology and the local optical properties of the rings, with simultaneous topographical and fluorescence images being obtained.[9] Fluorescence images of the rings themselves showed a strong correlation with the topography. An increase in fluorescence was accompanied by an equivalent increase in height (Figure 3b). To gain more insight into the optical properties of the rings, fluorescence polarization experiments were performed. Sets of images were acquired using linearly polarized light in both the horizontal and the vertical directions with respect to the image and with a polarizer in the emission path oriented parallel and perpendicular to the excitation direction. In the case of the rings which had not been annealed, no polarization effects were observed. In the case of the annealed rings, however, when the fluorescence intensity distribution in an individual ring (taking into account the height of the ring at each position) was compared with images acquired using respectively horizontally

(14) Ohara, P. C.; Heath, J. R.; Gelbart, W. M. *Angew. Chem., Int. Ed. Engl.* **1997**, *36*, 1078. Vossmeyer, T.; Chung, S.-W.; Gelbart, W. M.; Heath J. R. *Adv. Mater.* **1998**, *10*, 351.

(15) Liu, J.; Dai, H.; Hafner, J. H.; Colbert, D. T.; Smalley, R. E.; Tans, S. J.; Dekker, C. *Nature* **1997**, 780−781.

(16) Herwig, P.; Kayser, C. W.; Müllen, K.; Spiess, H. W.; *Adv. Mater.* **1996**, *8*, 511. Keegstra, M. A.; de Feyter, S.; De Schryver, F. C.; Müllen, K. *Angew. Chem., Int. Ed. Engl.* **1996**, *35*, 774; Tabushi, I.; Yamamura, K.; Okada, Y. *J. Org. Chem.* **1987**, *52*, 2502. Mollard, D. M.; Lillya, C. P. *J. Am. Chem. Soc.* **1989**, *111*, 1829.

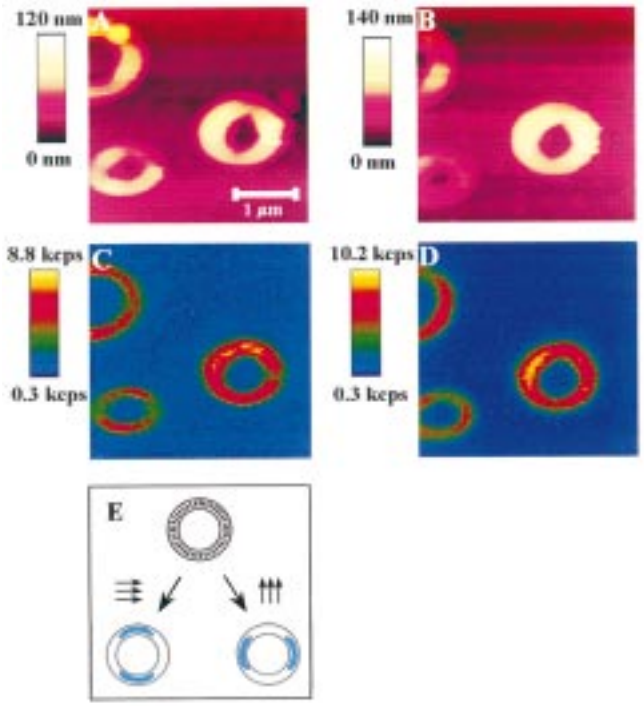

Figure 4. NSOM images of annealed rings of **5b** on a glass substrate taken with polarized laser light. Images A and B are topography images taken on the same region of the sample. Images C and D are fluorescence images simultaneously acquired with respective images A and B. The fluorescence image C is acquired using horizontally polarized light for excitation while detecting fluorescence light parallel to the excitation direction. Image D corresponds to the vertical polarization direction with parallel detection. The images were acquired using 514 nm as the excitation wavelength. Similar results were obtained using 458 nm as an excitation wavelength. Image E is a schematic representation of the polarized fluorescence emission of the ring-shaped aggregates upon polarized excitation as seen in A−D. Increased emission is observed at the top and bottom of the rings upon horizontal polarized light excitation and at the left and right sides of the ring upon vertical polarized light excitation. The fluorescence images indicate an ordered arrangement of molecules within the ring.

and vertically polarized excitation light, it was found that the fluorescence intensity at the upper and lower part of the ring was higher in the former case (horizontally polarized excitation light), while in the latter case (vertically polarized excitation light) the left and right part of the ring showed up brighter. This effect is clearly illustrated in parts A−D of Figure 4 and schematically shown in Figure 4E. (Fluorescence polarization images were also acquired with perpendicular excitation and detected polarization (not shown). In this case no difference in intensity between different parts of the ring could be observed.)

The correlation between the topology and fluorescence means that the fluorescence differences observed are due to a photoselection when linearly polarized excitation light is used, which leads to the conclusion that there must be a preferential orientation of the molecules with respect to their position in the ring. The observation that the photoselection occurs in the micrometer range indicates that there is significant order within the deposited material. From the fluorescence patterns, it can be concluded that at the top and bottom of a ring the porphyrin molecules are aligned orthogonal with respect to porphyrin molecules at the left or right side of a ring (or more correctly the transition dipole moments are orthogonal with respect to each other). When the excitation light is horizontal to the image, the molecules at the top and the bottom of the ring are preferentially excited because the transition dipole is aligned with the excitation field. In turn, the fluorescence can only be detected when the detection is parallel with the excitation configuration, suggesting that the absorption and emission dipoles are parallel. This effect can only occur if the porphyrin molecules are standing vertically within the rings and are oriented as shown in Figure 4E.

In the case of rings formed from molecule **1**,[9] order was only observed in the 50−100 nm range which corresponds to the size of the aggregate particles. The larger hexakis porphyrin molecule **5b** forms rings in an identical process to those formed by **1**; however, the larger porphyrin surface in molecule **5b** leads to an increase in intermolecular interactions which in turn results in a molecular ordering on a micrometer scale. The fact that, on average, larger rings are formed by molecule **5b** than by molecule **1** is also a result of this larger interaction. Although the rings are formed from a solution at room temperature, it can be postulated that the molecules have some preference to stack into columns when the thin film of the solution is concentrated by evaporation of the solvent. This effect is, however, not sufficiently strong enough to induce ordering within the ring. Upon annealing, the molecules or aggregates of molecules within the ring become more ordered. The combination of these two self-assembling processes, the physical phenomenon of bubble formation[8] (or wetting−dewetting behavior)[9] which directs the porphyrin to self-assemble into a circular geometry and the ordering due to annealing, working in tandem results in both larger rings and in increased molecular order within the rings.

This exciting result can be used as a lead for the further design of functional synthetic analogues of the naturally occurring light-harvesting complexes and the formation of potential molecular photovoltaic devices.

Experimental Section

Materials. Hexakis(bromomethyl)benzene, 1,2 dibromomethylbenzene, and bromoxylene were all purchased from Aldrich and were used without further purification. All solvents were predried before use.

Methods. ^{1}H NMR spectra were recorded on Bruker WM-200 and Brucker AM-400 instruments. Chemical shifts are reported in ppm downfield from internal $(CH_3)_4Si$. Standard Bruker 2D pulse programs (COSY-DQF, COSYDFTP, and NOESY) were used for structural assignments; 0.75 s was used as a mixing time for all NOESY experiments. FAB-MS spectra were recorded on a VG 7070E instrument; the matrix used was 3-nitrobenzyl alcohol. Electron spray MS was recorded using a Perkin-Elmer-Sciex API 300 mass spectrometer with a mass range of 3000. Field desorption (FD) was carried out using a JEOL JMS SX/SX102A four-sector mass spectrometer, coupled to a JEOL MS-MP7000 data system. For the NSOM measurements see ref 9.

Synthesis. The synthesis of the porphyrin precursors **2a** and **2b** was carried out according to literature procedures.[17] The copper-containing porphyrin compounds **Cu·3**, **Cu·4**, **Cu·5**, were prepared from the respective free-base derivatives **3**, **4**, **5b**, and copper acetate according to a standard proceedure.[18] All derivatives were characterized by MALDI-TOF-MS, melting points, and elemental analysis.

Monoporphyrin 3. To a solution of 283 mg (0.18 mmol) of porphyrin **2b** in 20 mL of dry DMF was added 21.4 mg (0.18 mmol) of benzyl bromide and 100 mg of K_2CO_3. The mixture was refluxed overnight. The product was extracted with dichloromethane and washed with water. After evaporation of the solvent, the resulting product was purified by flash column chromatography (Silica 60H, eluent, CH_2Cl_2, $R_f = 0.9$). A red solid was obtained in 44% yield: ^{1}H NMR ($CDCl_3$,

(17) Little, R. G.; Anton, J. A.; Loach, P. A.; Ibers, J. A. *J. Heterocycl. Chem.* **1975**, *12*, 343.

(18) Buchler, J. W. *The Porphyrins*; Dolphin, D., Ed., Academic Press: NY, 1978; Vol. 1, Chapter 10, p 389.

300 MHz) $\delta = 8.86$ (s, 8 H, pyrrolic H), 8.12 (d, 2 H, phenyl H), 8.11 (d, 6 H, phenyl H), 7.7−7.38 (m, 5 H, 6-ArH porphyrin), 7.35 (d, 2 H, phenyl H), 7.27 (d, 6 H, phenyl H), 5.34 (s, 2 H, benzylic CH_2), 4.24 (t, 6 H, O*CH*$_2$CH$_2$, $J = 6.5$ Hz), 2.0 (m, 6 H, OCH$_2$*CH*$_2$), 1.6−1.1 (br m, 78 H, CH_2 (tails)), 0.87 (t, 9 H, CH_3), −2.74 (s, 2 H, NH); formula $C_{99}H_{133}N_4O_4$ calculated 1442.03; ES-MS *m*/*z* 1442.3 [M^+], 721.8 [M^{2+}]; UV−vis ($CHCl_3$, λ/nm (log ϵ/dm^3 mol^{-1}cm^{-1})) 422.6 (6.75), 519.1 (5.30), 556.8 (5.16), 592.6 (4.82), 650.4 (4.88). Anal. Calcd for $C_{99}H_{133}N_4O_4$: C, 82.39; H, 9.29; N, 3.88. Found: C, 82.36; H, 9.22; N, 3.98.

Bis Porphyrin 4. To a solution of 112 mg (0.074 mmol) of porphyrin **2b** in 20 mL of dry DMF was added 11.0 mg (0.037 mmol) of α,α′-dibromooxylene and 50 mg of K_2CO_3. The mixture was refluxed overnight. After work up as described for **3**, a red solid was obtained in 49% yield: mp 109 °C; ^{1}H NMR ($CDCl_3$, 300 MHz) $\delta =$ 8.81 (d, 4 H, pyrrolic H), 8.74 (d, 4 H, pyrrolic H), 8.62 (d, 4 H, pyrrolic H), 8.22 (d, 2 H, phenyl H), 8.20 (d, 4 H, phenyl H), 8.10 (d, 4 H, phenyl H), 7.78 (d of d, 2 H, xylyl), 7.59 (d of d, 2 H, xylyl), 7.45 (d, 4 H, phenyl H), 7.28 (d, 4 H, phenyl H), 7.22 (d, 8 H, phenyl H), 6.33 (d, 8 H, phenyl H), 5.67 (s, 4 H, benzylic CH_2), 4.25 (t, 4 H, O*CH*$_2$-CH$_2$, $J = 6.4$ Hz), 3.50 (t, 8 H, O*CH*$_2$CH$_2$, $J = 6.4$ Hz), 2.0 (m, 6 H, OCH$_2$*CH*$_2$), 1.6−1.1 (br m, 168 H, CH_2 (tails)), 0.87 (m, 18H, CH_3), −2.75 (s, 4H, NH); $C_{192}H_{258}N_8O_8$ calculated mass 2806.2; ES-MS *m*/*z* 2807.1 [M^+H], 1403.9 [M^{2+}H]; UV−vis ($CHCl_3$, λ/nm, (log ϵ/dm^3 mol^{-1}cm^{-1})) 422.9 (6.84), 519.31 (5.53), 556.4 (5.37), 594.2 (5.08), 649.0 (5.18). Anal. Calcd for $C_{192}H_{258}N_8O_8$: C, 82.17; H, 9.27; N, 4.00. Found: C, 82.05; H, 9.19; N, 4.07.

Hexakis Porphyrin 5a. To a solution of 100 mg (0.15 mmol) of porphyrin **2a** in 4 mL of dry DMF was added 15.7 mg (0247 mmol) of hexakis(bromomethyl)benzene and 100 mg of K_2CO_3. The mixture was stirred overnight at 50 °C. The reaction mixture was poured into water and extracted with dichloromethane. The organic layer was evaporated to dryness. The resulting product was purified by column chromatography (eluent CH_2Cl_2, $R_f = 0.9$). A purple solid was obtained in 30% yield: ^{1}H NMR ($CDCl_3$, 400 MHz) $\delta = 8.86$ (d, 12 H, pyrrolic H), 8.83 (d, 12 H, pyrrolic H), 8.59 (d, 12 H, pyrrolic H), 8.33 (d, 12 H, phenyl H), 8.21 (d, 12 H, phenyl H), 8.21 (d, 4 H, pyrrolic H), 8.11 (d, 12 H, phenyl H), 7.54 (d, 12 H, phenyl H), 7.16 (d, 24 H, phenyl H), 6.47 (d, 24 H, phenyl H), 5.89 (s, 12 H, benzylic CH_2), 2.68 (m, 18 H, CH_3), 2.05 (m, 36 H, CH_3), −2.72 (s, 4 H, NH); $C_{294}H_{222}N_{24}O_6$ calculated mass 4178.78; ES-MS *m*/*z* 698.54 [M^{6+}], 838.52 [M^{5+}], 1048.03 [M^{4+}], 1397.05 [M^{3+}]; estimated mass 4187.25 [−2.94 for C-isotope]; UV−vis ($CHCl_3$, λ/nm) 422.9, 519.0, 556.0, 593.4, 650.2.

Hexakis Porphyrin 5b. To a solution of 356 mg (0.26 mmol) porphyrin **2b** in 20 mL of dry DMF was added 22 mg (0.035 mmol) of hexakis(bromomethyl)benzene and 200 mg of K_2CO_3. The mixture was refluxed overnight. The product was extracted with dichloromethane and washed with water. After workup as described for **5a**, the resulting product was purified by column chromatography (Silica 60H, eluent $CHCl_3$/Hexane 7:3 v/v, $R_f = 0.9$). A red solid was obtained in 34% yield: mp 185 °C; ^{1}H NMR ($CDCl_3$, 300 MHz) $\delta = 8.86$ (d, 12 H, pyrrolic H), 8.81 (d, 12 H, pyrrolic H), 8.50 (d, 12 H, pyrrolic H), 8.46 (d, 12 H, phenyl H), 8.14 (d, 12 H, phenyl H), 7.98 (d, 4 H, pyrrolic H), 7.78 (d, 12 H, phenyl H), 7.30 (d, 12 H, phenyl H), 6.74 (d, 24 H, phenyl H), 5.72 (d, 24 H, phenyl H), 6.22 (s, 12 H, benzylic CH_2), 4.28 (t, 12 H, O*CH*$_2$CH$_2$, $J = 6.4$ Hz), 2.94 (t, 24 H, O*CH*$_2$CH$_2$, $J = 6.4$ Hz), 2.0 (m, 24 H, OCH$_2$*CH*$_2$), 1.6−1.1 (br m, 504 H, CH_2 (tails)), 0.88 (m, 54 H, CH_3), −2.65 (s, 4H, NH); $C_{564}H_{762}N_{24}O_{24}$ calculated mass 8262.40; ES-MS: 8266.73 [M^+], 698.54 [M^{6+}], 1378.81 [M^{5+}], 1653.74 [M^{4+}], 2067.71 [M^{3+}]; UV−vis ($CHCl_3$, λ/nm, log(ϵ/dm^3 mol^{-1}cm^{-1})) 422.9 (7.00), 518.9 (6.80), 556.5 (6.30), 593.2 (5.90), 650.5 (5.90). Anal. Calcd for $C_{564}H_{762}N_{24}O_{24}$: C, 81.98; H, 9.30; N, 4.07. Found: C, 81.89; H, 9.46; N, 4.01.

Acknowledgment. This work was supported by FWO and DWTH through IUAP-4-11.

Supporting Information Available: Table S1 (^{1}H NMR chemical shifts), Figure S2 (NOE interactions) (2 pages, print/PDF). See any current masthead page for ordering information and Web access instructions.

JA9815632